Planta (2024) 260:144
https://doi.org/10.1007/s00425-024-04572-2

ORIGINAL ARTICLE

The origin and metabolic fate of 4-hydroxybenzoate in Arabidopsis

Zhaniya Batyrshina[1] · Anna K. Block[2] · Gilles J. Basset[1]

Received: 12 August 2024 / Accepted: 8 November 2024

Abstract

Main conclusion **The contribution of *p*-coumarate *β*-oxidation and kaempferol cleavage to the pools of glycosylated, free and cell wall-bound 4-hydroxybenzoate is organ-dependent in Arabidopsis.**

Abstract 4-Hydroxybenzoate (4-HB) is a vital precursor for a number of plant primary and specialized metabolites, as well as for the assembly of the plant cell wall. In Arabidopsis, it is known that 4-HB is derived independently from phenylalanine and tyrosine, and that the metabolism of phenylalanine into 4-HB proceeds via at least two biosynthetic routes: the *β*-oxidation of *p*-coumarate and the peroxidative cleavage of kaempferol. The precise contribution of these precursors and branches to 4-HB production, however, is not known. Here, we combined isotopic feeding assays, reverse genetics, and quantification of soluble (i.e., free and glycosylated) and cell wall-bound 4-HB to determine the respective contributions of phenylalanine, tyrosine, *β*-oxidation of *p*-coumarate, and peroxidative cleavage of kaempferol to 4-HB biosynthesis in Arabidopsis tissues. Over 90% of 4-HB was found to originate from phenylalanine in both leaves and roots. Soluble 4-HB level varied significantly between organs, while the proportion of cell wall-bound 4-HB was relatively constant. In leaves and flowers, glycosylated and cell wall-bound 4-HB were the most and least abundant forms, respectively. Flowers displayed the highest specific content of 4-HB, while free 4-HB was not detected in roots. Although *p*-coumarate *β*-oxidation and kaempferol catabolism were found to both contribute to the supply of 4-HB in all tissues, the proportion of kaempferol-derived 4-HB was higher in roots than in leaves and flowers. Within the *β*-oxidative branch, *p*-coumaroyl-CoA ligase 4-CL8 (At5g38120) bore a preponderant role in the production of soluble and cell wall-bound 4-HB in leaves, while *p*-coumaroyl-CoA ligase At4g19010 appeared to control the biosynthesis of soluble 4-HB in flowers. Furthermore, analysis of a series of Arabidopsis T-DNA mutants corresponding to the three major UDP-glucosyltransferases known to act on 4-HB in vitro (UGT75B1, UGT89B1, and UGT71B1) showed that none of these enzymes appeared in fact to have a significant role in the glycosylation of 4-HB in vivo.

Keywords 4-Hydroxybenzoate · Phenolics · Phenylpropanoids · Kaempferol · Ubiquinone · *p*-Coumaroyl-CoA ligases · UDP-glucosyltransferases

Abbreviations

4-HB 4-Hydroxybenzoate
UGTs UDP-glucosyltransferases

Communicated by Stefan de Folter.

✉ Zhaniya Batyrshina
zh.batyrshina@ufl.edu

✉ Gilles J. Basset
gbasset@ufl.edu

[1] Plant Molecular & Cellular Biology Program, Department of Horticultural Sciences, University of Florida, 1109 Fifield Hall, P.O. Box 110690, Gainesville, FL 32611, USA

[2] Center for Medical, Agricultural and Veterinary Entomology, ARS, USDA, Gainesville, FL 32608, USA

Introduction

4-Hydroxybenzoate (4-HB) is an essential phenolic compound that serves as a component of the plant cell wall (e.g., lignin decoration and sporopollenin assembly) as well as a ring precursor for the biosynthesis of the respiratory cofactor and antioxidant ubiquinone (Coenzyme Q) (Xue et al. 2020; Goacher et al. 2021; Berger et al. 2022). Moreover, some members of the Boraginaceae family use 4-HB as a precursor for the biosynthesis of some specialized naphthoquinones called shikonins (Yazaki 2017; Suttiyut et al. 2023).

There has been long standing interest in 4-HB as a target molecule for plant metabolic engineering, both to boost ubiquinone level in crops and as an alternative to petrochemical synthesis for the production of antimicrobials,

Published online: 19 November 2024

pharmaceuticals, and copolyesters (Siebert et al. 1996; Viitanen et al. 2004; Soubeyrand et al. 2021; Mottiar et al. 2023). Yet, in spite of its biological and biotechnological significance, the metabolism of 4-HB in plant cells is far from being fully understood. In fact, the enzymatic architecture of 4-HB biosynthesis is known mainly from indirect studies aimed at elucidating the biosynthesis of some of its downstream products, such as ubiquinone and shikonins (Block et al. 2014; Soubeyrand et al. 2018, 2019; Nakanishi et al. 2024). For instance, reverse genetics have shown that in Arabidopsis about half of the benzenoid moiety of ubiquinone originates from the *β*-oxidation of *p*-coumarate in peroxisomes via, most likely, the formation of 4-HB (Fig. 1). In this pathway, 4-hydroxybenzoate must be exported from peroxisomes and imported into mitochondria where ubiquinone biosynthesis takes place (Fig. 1; Berger et al. 2022). Similarly, in *Lithospermum erythrorhizon*, two functionally redundant *p*-coumaroyl-CoA ligases, which are located in peroxisomes, control most of the production of shikonin (Nakanishi et al. 2024). In Arabidopsis and tomato, it is also known that the peroxidative cleavage of kaempferol supplies 20–25% of 4-HB that serves as a precursor for ubiquinone's benzenoid moiety (Fig. 1).

There are reasons, however, to suspect that in Arabidopsis and other plant species the respective contributions of the metabolism of *p*-coumarate and that of kaempferol to ubiquinone biosynthesis might not quantitatively correlate with the production of 4-HB. First, ubiquinone is a trace cofactor, the pool size of which is dwarfed by that of its benzenoid precursors (Soubeyrand et al. 2018, 2021). Large variations in ubiquinone content could, therefore, occur between tissues or in response to changes in environmental conditions, while 4-HB biosynthetic fluxes and pool sizes remain constant. Second, extensive deposits of 4-HB are known to occur as glycosylated conjugates in plant vacuoles (Siebert et al. 1996; Cooper-driver et al. 1972; Yazaki et al. 1995), and into lignin polymers via ester linkage (Lu et al. 2015; Rencoret et al. 2020; Mottiar et al. 2023). It is conceivable that only part -or possibly even none- of such sequestered 4-HB might be reclaimable for ubiquinone biosynthesis. Compounding the difficulty to establish quantitative correlations between the biosynthesis of ubiquinone and that of its aromatic precursors, isotope labeling assays have shown that Arabidopsis can also derive the benzenoid moiety of ubiquinone from the ring of tyrosine (Block et al. 2014; Fig. 1). It is not known, however, if in plants this alternative pathway entails the formation of 4-HB (Block et al. 2014).

Materials and methods

Chemical and reagents

[*ring*-$^{13}C_6$]-L-Phenylalanine and [*U*-$^{13}C_9$-^{15}N]-L-tyrosine were from Cambridge Isotope Laboratories Inc. Murashige and Skoog (MS) medium was from MP Biomedicals, LLC. 4-Hydroxybenzoate was from Acros Organics; standards were prepared in 0.1 N HCl and quantified spectrophotometrically using the extinction coefficient of 13,900 M^{-1} cm^{-1} at

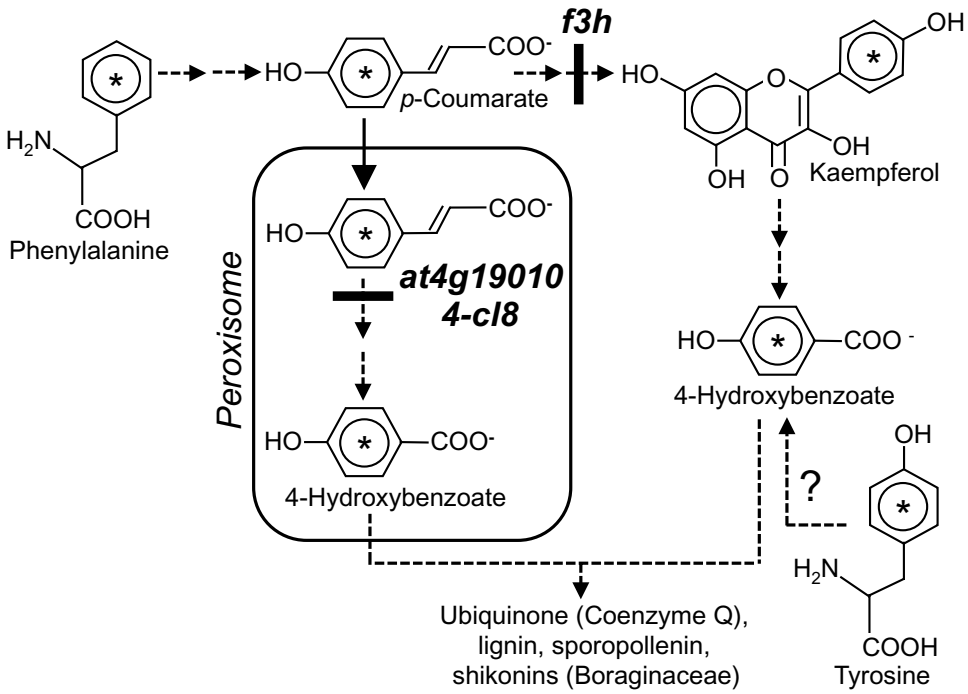

Fig. 1 Overview of the metabolic routes yielding 4-HB in plant cells. Black bars symbolize the metabolic blockages corresponding to the Arabidopsis mutants used in the present study, i.e., cytosolic *flavanone-3-hydroxylase* (*f3h*) in the flavonoid biosynthetic pathway, and two peroxisomal *4-coumaroyl-CoA ligases* (*at4g19010* and *4-cl8*) involved in the *β*-oxidative metabolism of *p*-coumarate. Dashed arrows symbolize multiple steps. Note that in plants the usage of tyrosine as an early precursor of 4-HB is hypothetical

255 nm (Dawson et al. 1986). Unless otherwise mentioned, other chemicals and reagents were from Fisher Scientific.

Plant material and growth conditions

Arabidopsis T-DNA insertion lines *at4g19010* (*at4g19010*; SALK_043310), *4-cl8* (*at5g38120;* SALK_137753), and *f3h* (*at3g51240;* SALK_113321) were those described and confirmed as genuine knockout alleles in Block et al. (2014), Soubeyrand et al. (2019) and Masini (2014), respectively. The *at4g19010*×*f3h* and *at4g19010*×*4-cl8* double mutants were those generated by Soubeyrand et al. (2019). Lines *ugt75b1* (*at1g05560*; SALKseq_063933), *ugt89b1* (*at1g73880*; SAIL_1173_C09), and *ugt71b1* (*at3g21750*; SAIL_846_BO6) were obtained from the Arabidopsis Biological Resource Center (Alonso et al. 2003). T-DNA homozygosity was verified via PCR-genotyping using the following line specific primers: RP 5′-TGATGAGAATTT TCGGTTTGG-3′ and LP 5′-AATGGTCTCAATTACCTG TTGC-3′ for SALKseq_063933, RP 5′-AGGCAAATGAAG AGTTGGAGC-3′ and LP 5′-GAATCTTGCAGCGCAAGT AAG-3′ for SAIL_1173_C09, and RP 5′-GAAGCGTTG GACGTGTAGAAG-3′ and LP 5′-GCAATTTCAACAGAG AGACGC-3′ for SAIL_846_BO6. T-DNA-specific primers were LBb1.3 5′-ATTTTGCCGATTTCGGAAC-3′ (SALK) and LB1 5′-GCCTTTTCAGAAATGGATAAATAGCCT TGCTTCC-3′ (SAIL). Total RNAs were prepared from rosette leaves using the RNeasy Plant Mini Kit (Qiagen) and quantified by absorbance at 260 nm. cDNAs were generated with the ImProm-IITM Reverse Transcription System (Promega). PCR amplifications were performed using the following primers pairs: 5′-ACTTCAGTGGAGCTAAGA CAAGT-3′ (forward) and 5′-ACTCCATCATTTCTTGAA ACGCA-3′ (reverse) for *UGT75B1*, 5′-CCTTTTCCCTCC CACCCTTC-3′ (forward) and 5′-GGTTATCCTCACGTG CGTCA-3′ (reverse) for *UGT89B1*, 5′-TGTGTTCATACC ATCGCCGG-3′ (forward) and 5′-TCCATGTCAGCCACC GAATT-3′ (reverse) for *UGT71B1*, and 5′-CTAAGCTCT CAAGATCAAAGGC-3′ (forward) and 5′-TTAACATTG CAAAGAGTTTCAAGG-3′ (reverse) for the actin control. For metabolite analyses, rosette leaves were collected on 4-week-old Arabidopsis plants grown on potting mix at 22 °C in 12-h days at 160 µE m^{-2} s^{-1} and then transferred to 16-h days at 600 µE m^{-2} s^{-1} 3 days prior to harvesting. Flower buds were harvested from 8-week-old plants. For root tissue, Arabidopsis seeds were germinated on MS agar plates containing 1% (*w*/*v*) sucrose. Three-day-old seedlings were transferred to MS liquid medium supplemented with 1% (*w*/*v*) sucrose and cultured for 2 weeks on an orbital shaker (60 rpm) at 22 °C and protected from light. For heavy isotope labeling assays, Arabidopsis Col-0 seeds were germinated on MS agar plates containing 1% sucrose (*w*/*v*). Seven-day-old seedlings were then transferred to MS liquid medium containing 1% sucrose and grown for 10 days on orbital shaker in 12-h light photoperiod (160 µE m^{-2} s^{-1}). Labeling was conducted for 3 h and 6 h using 250 µM doses of [*ring*-$^{13}C_6$]-L-phenylalanine or [*U*-$^{13}C_9$-^{15}N]-L-tyrosine.

Extraction and analyses of 4-HB and kaempferol

Leaf, flower and root tissues (~ 100 mg) were homogenized in 300 µl of methanol:water (90:10, v/v) using a 5 ml Pyrex tissue grinder. The grinder was washed twice with 300 µl of methanol:water (90:10, v/v), washes were combined with the original extract, and the samples were cleared by centrifugation (5 min; 21,000×*g*). Pellets were set aside for the analyses of cell wall-bound 4-HB (see below). Supernatants were then divided into two aliquots (2 × 300 µl), which were mixed with 100 µl of freshly prepared 75 mM ascorbic acid and 350 µl of 3 N HCl. For the quantification of free 4-HB, 400 µl of the first aliquot was immediately phase-partitioned using 1 ml of 100% ethyl acetate and vortexing for 1 min. Phases were separated (2 min; 21,000×*g*) and the ethyl acetate-containing fraction was evaporated to dryness. Samples were resuspended for 10 min at room temperature in 300 µl of 0.1 N HCl and 30 µl of 75 mM ascorbic acid. Total 4-HB was quantified in the second aliquot after deglucosylation via acid hydrolysis (70 °C for 1 h). Samples were then processed as described for the first aliquot. For the analysis of cell wall-bound 4-HB, pellets from the initial potter extraction were washed 3 times with 1 ml of methanol:water (90:10, v/v) and vortexing. No soluble 4-HB was detected by the second wash. Washed pellets were resuspended in 1 ml of 2 M NaOH and incubated for 24 h at 30 °C. Samples were then neutralized with 400 µl of 6 N HCL at 4 °C and cleared by centrifugation (5 min; 21,000×*g*). Sample aliquots (400 µl) were then phase partitioned, evaporated to dryness, and resuspended in 300 µl of 0.1 N HCl and 30 µl of 75 mM ascorbic acid as described above. Samples were centrifuged (5 min; 21,000×*g*) prior to injection (50 µl) on an Agilent Technologies Zorbax Eclipse Plus C18 column (4.6 × 100 mm; 3.5 µm) held at 30 °C. The column was developed isocratically at a flow rate of 0.8 ml min^{-1} with a mobile phase containing 95% of 10 mM sodium acetate (pH 3.5) and 5% (v/v) methanol. 4-HB (13.8 min) was monitored via diode array spectrophotometry and quantified according to external calibration standards at 255 nm. Amounts of glycosylated 4-HB were calculated by subtracting the amounts measured in acid-hydrolyzed samples (total 4-HB) from the amounts measured in the corresponding samples not subjected to acidic hydrolysis (free 4-HB). Total kaempferol was quantified in the same acid-hydrolyzed extracts used for total 4-HB analysis, prior to the partitioning step. Samples were centrifuged (5 min; 21,000×*g*) and then injected (10 µl) on an Agilent Technologies Zorbax Eclipse Plus C18 column (4.6 × 100 mm; 3.5 µm) held at 30 °C. The column

was developed at a flow rate of 0.8 ml.min^{-1} using a 25-min linear gradient starting with 95% of 10 mM sodium acetate (pH 3.5) and 5% (v/v) methanol and ending with 100% (v/v) methanol. Kaempferol eluted at 17.8 min and was quantified spectrophotometrically (365 nm) according to external calibration standards.

For liquid chromatography–tandem mass spectrometry analyses, 5 µl of extracts was chromatographed on an Agilent Technologies Eclipse Plus C18 RRHD column (2.1 × 50 mm; 1.8 µm) held at 30 °C and using solvent A [0.1% (v/v) formic acid in water] and solvent B [0.1% (v/v) formic acid in methanol] at a flow rate of 0.4 ml min^{-1}. The separation gradient was isocratic at 5% of solvent B for 0.5 min, then increased to 100% of solvent B over 5.5 min, isocratic at 100% of solvent B for 1 min, then a returned to 5% of solvent B over 0.1 min and isocratic at 5% of solvent B over 2.9 min. 4-HB eluted at 3.75 min in this system. The eluate was electrosprayed in negative mode (2500 V) into a Thermo Scientific TSQ Quantis instrument. Ion transfer tube temperature was 300 °C, vaporizer temperature was 350 °C, and collision energy was 53.95 V. Single reaction monitoring (SRM) was used to quantify labeled and unlabeled 4-HB using the following ion pairs in negative scan mode: 4-HB (137.02–93.05 *m/z*), [$^{13}C_6$]-4HB (143.02–99.05 *m/z*), and [$^{13}C_7$]-4HB (144.02–99.05 *m/z*).

Results and discussion

Arabidopsis leaf and root tissues derive most of their 4-HB from phenylalanine

We first sought to determine if in plant tissues tyrosine served as a biosynthetic precursor of 4-HB, and if so what the contribution of this amino acid was as compared to that of phenylalanine. To do that, identical doses of ring ^{13}C-labeled phenylalanine and uniformly ^{13}C-labeled tyrosine were fed to axenic cultures of Arabidopsis; the isotopic enrichment of 4-HB was then quantified via liquid chromatography–tandem mass spectrometry. Direct incorporation of phenylalanine and tyrosine—i.e., without intramolecular isotopic dilution—into 4-HB could be accurately monitored owing to the specific carbon labeling profile associated with each amino acids: [*Ring*-$^{13}C_6$]-Phenylalanine and [*U*-$^{13}C_9$;^{15}N]-Tyrosine being predicted to generate [*Ring*-$^{13}C_6$]-4-HB and [*U*-$^{13}C_7$]-4-HB, respectively (Fig. 2). Labeling of soluble and cell wall-bound 4-HB from phenylalanine was readily detected in both rosette leaves and roots (Fig. 2a). Within 6 h of labeling, the rate of isotopic enrichment of soluble 4-HB was 13 to 23 times that of cell wall-bound 4-HB in leaves and roots, respectively (Fig. 2a; Table 1). The rate of isotopic enrichment of 4-HB from phenylalanine was also markedly higher in roots as compared to that in leaves, the difference between these organs ranging from 3.7- to 6.4-fold for soluble and cell wall-bound 4-HB, respectively (Fig. 2a; Table 1). In contrast, no labeling of soluble 4-HB from tyrosine was detected in either leaves or roots (Fig. 2b). Low levels of tyrosine incorporation were detected in cell wall-bound 4-HB (Fig. 2a). The corresponding rates of isotopic enrichment were similar to those measured from phenylalanine, and here again were higher (~ 4 times) in roots than in leaves (Fig. 2a; Table 1). Juxtaposing the rates of isotopic enrichment with the total—i.e., labeled and unlabeled—pool sizes of 4-HB highlights the observation that, in Arabidopsis, the bulk of 4-HB (98% in leaves and 92% in roots) originates directly from phenylalanine (Fig. 2c). This result contrasts sharply with the situation observed in yeast and animals, which produce 4-HB via the formation of 4-hydroxyphenyl pyruvate and tyrosine (Pierrel 2017). Also notable is the difference between the contribution of tyrosine to the biosynthesis of 4-HB as compared to that of ubiquinone. Previous work indicated indeed that tyrosine supplied about 30% of the aromatic precursor of ubiquinone's benzenoid moiety in both leaf shoots and roots (Block et al. 2014). One can, therefore, infer that either it exists a pool of tyrosine-derived 4-HB that is dedicated to ubiquinone production (e.g., via sequestration in mitochondria where ubiquinone assembly takes place), or that in plants the usage of tyrosine as a precursor for ubiquinone's ring does not proceed via the formation of 4-HB.

The β-oxidative metabolism of *p*-coumarate and peroxidative cleavage of kaempferol both contribute to the supply of 4-HB throughout *Arabidopsis* tissues

Having shown that in Arabidopsis 4-HB is primarily derived from phenylalanine, we sought to quantify the contribution of each of the known downstream branches, namely *β*-oxidation of *p*-coumarate and peroxidative catabolism of kaempferol (Fig. 1). Five Arabidopsis T-DNA knockouts were selected for these experiments: *at4g19010* and *4-cl8*, which correspond to two 4-coumaroyl-CoA ligases involved in the *β*-oxidation of *p*-coumarate (Block et al. 2014; Soubeyrand et al. 2019); *at4g19010* × *4-cl8*, a cognate double knockout (Soubeyrand et al. 2019); *f3h*, which corresponds to flavanone-3-hydroxylase of the core flavonoid biosynthetic pathway (Masini 2014)), and last an *at4g19010* × *f3h* double knockout (Soubeyrand et al. 2019). These five Arabidopsis mutants have been shown to display reduced incorporation of phenylalanine into ubiquinone in rosette leaves; this incorporation of phenylalanine being the lowest in *at4g19010*, *at4g19010* × *4-cl8*, and *at4g19010* × *f3h* (Soubeyrand et al. 2019). Figure 1 shows the locations of the corresponding alleles in the context of phenylpropanoid and ubiquinone metabolism. Here, the

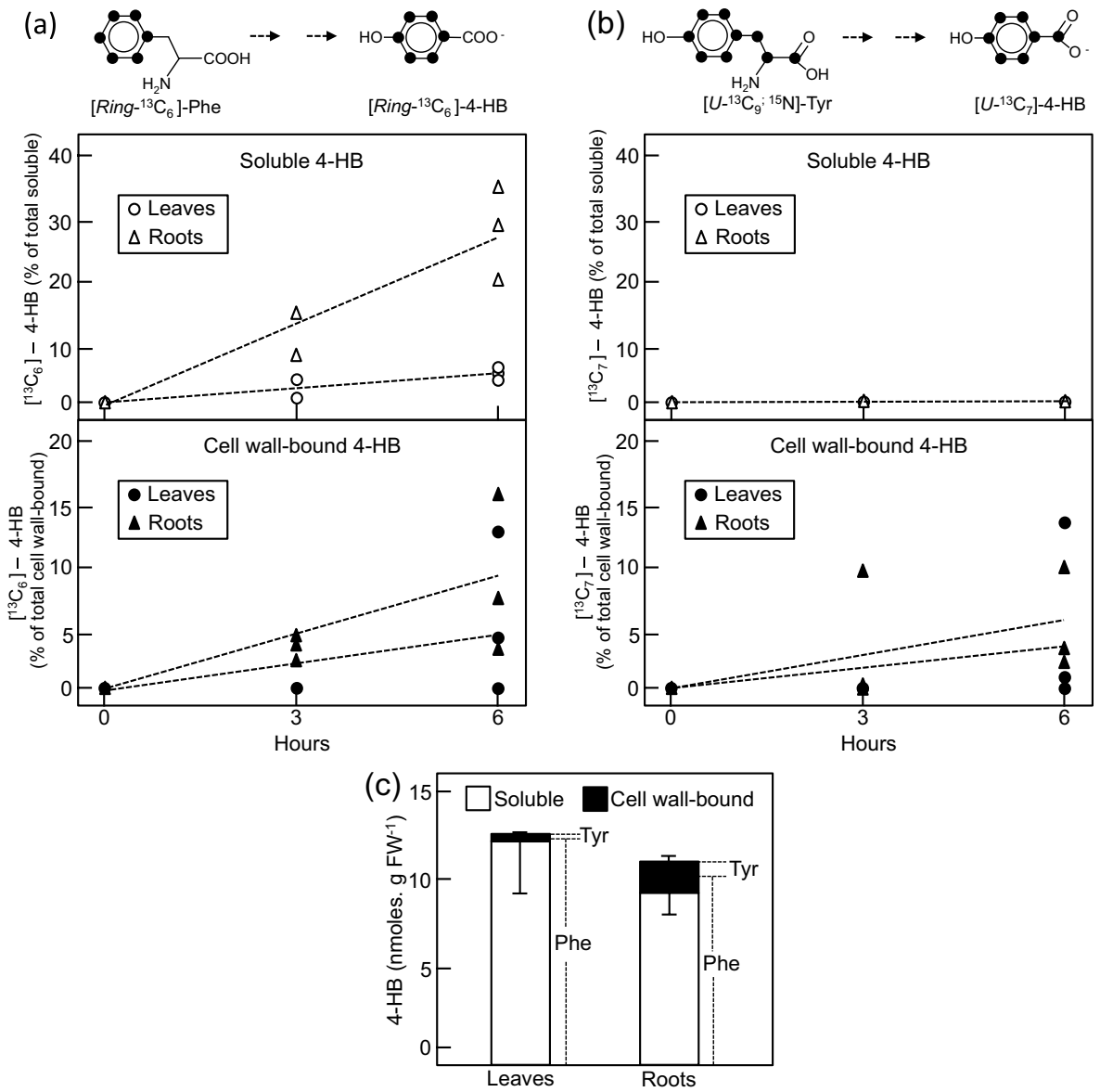

Fig. 2 Isotopic feeding assays in axenic cultures of Arabidopsis. **a** Soluble and cell wall-bound [*Ring*-$^{13}C_6$]-4-HB content in the rosette leaves and roots of Columbia-0 Arabidopsis plants fed for 3 and 6 h with 250 µM doses of [*Ring*-$^{13}C_6$]-Phenylalanine. **b** Soluble and cell wall-bound [*U*-$^{13}C_7$]-4-HB content in the rosette leaves and roots of Columbia-0 Arabidopsis plants fed for 3 and 6 h with 250 µM doses of [*U*-$^{13}C_9$;^{15}N]-Tyrosine. **c** Respective contribution of phenylalanine and tyrosine to the total content of soluble and cell wall-bound 4-HB in Arabidopsis rosette leaves and roots

Table 1 Rate of 4-HB labeling

	(nmoles.mg FW^{-1}. h^{-1})	
	Soluble	Cell-wall bound
[$^{13}C_6$]-Phe		
Leaves	0.1156 ± 0.0173	0.005 ± 0.003
Roots	0.4286 ± 0.074	0.0318 ± 0.02
[$^{13}C_9$]-Tyr		
Leaves	–	0.0057 ± 0.005
Roots	–	0.0206 ± 0.009

Values are from 3 replicates ± SE

pools of soluble and cell wall-bound 4-HB were analyzed in rosette leaves, flowers, and roots (Fig. 3). The soluble pool itself was scrutinized further in order to quantify the proportions of glycosylated and free forms of 4-HB. Total 4-HB levels are provided in Table S1.

In wild-type flowers and leaves, glycosylated and cell wall-bound 4-HB were consistently the most and least abundant forms, respectively (Fig. 3a-c). Free 4-HB was not detected in roots (Fig. 3c). Flowers displayed the highest specific content of 4-HB; the level of total 4-HB corrected for fresh weight representing in flowers ~ 3 times that of leaves

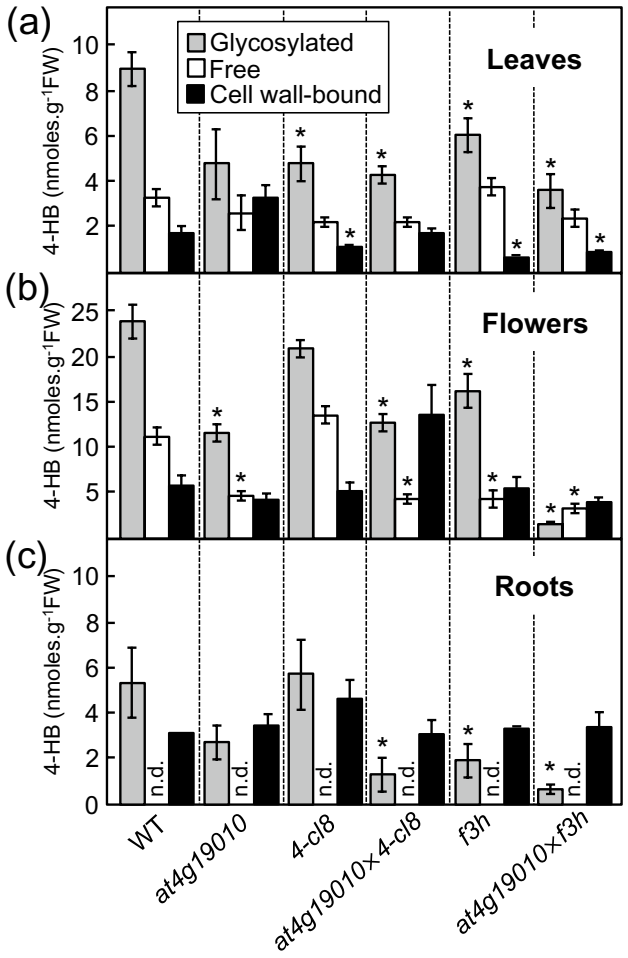

Fig. 3 Content in glycosylated, free, and cell wall-bound 4-HB in Arabidopsis tissues. **a** Leaves; **b** flowers; **c** roots. Data represent the means of 4–5 biological replicates ± SE. Asterisks indicate significant differences from the wild-type control as determined by Fisher's test ($p < 0.1$) from an analysis of variance

and ~ 5 times that of roots (Fig. 3a-c). In rosette leaves, all mutants displayed lower levels of glycosylated 4-HB as compared to the wild-type reference, the decrease ranging from 34% in the *f3h* knockout to 62% in the *at4g19010*×*f3h* double knockout (Fig. 3a). In the *at4g19010* leaf tissues, however, such a decrease was not statistically significant ($p = 0.15$; Fig. 3a). Lower levels of cell wall-bound 4-HB were observed only for the *4-cl*8, *f3h*, and *at4g19010*×*f3h* mutants; the decrease representing ~ 50% of the wild-type level in these last two lines (Fig. 3a). No statistically significant difference in the content of free 4-HB was observed for any of the mutants (Fig. 3a). In flowers, significant decreases in glycosylated and free 4-HB were associated with the loss of function of At4g19010 and F3H, but not that of 4-CL8 (Fig. 3b). Stacking of the *at4g19010* and *f3h* alleles resulted in the most severe impact on soluble 4-HB; as compared to wild-type, the flowers of the *at4g19010*×*f3h* double knockout displayed decreases of 92% and 63% in glycosylated and free 4-HB content, respectively (Fig. 3b). None of the mutants displayed any statistically significant difference in the content of cell wall-bound 4-HB (Fig. 3b). In roots, statistically significant differences in 4-HB level were restricted to its glycosylated form, and were observed only in the *at4g19010*×*4-cl8*, *f3h*, and *at4g19010*×*f3h* mutants (Fig. 3c). The most severe decrease in 4-HB level was observed in the *at4g19010*×*f3h* double knockout, the glycosylated 4-HB content of which was only a tenth of that of wild-type root tissues (Fig. 3c). One should also note that here again our data reveal some divergences between the biosynthesis of 4-HB and its usage for ubiquinone assembly. In particular, while the 4-CL8 and F3H-dependent branches have been shown to have accessory contributions as compared to that controlled by At4g19010 when the corresponding knockout mutants were scored for ubiquinone content (Soubeyrand et al. 2018; 2019), they were found here to be major contributors to total leaves 4-HB production (Table S1).

None of the major *Arabidopsis* UDP-glucosyltransferases known to act on 4-HB in vitro appears to play a predominant role in the glycosylation of 4-HB in vivo

In vitro activity screening of the members of the Arabidopsis UDP-glucosyltransferases (UGTs) family identified eight recombinant versions that acted on 4-HB (Lim et al. 2002). Three of those stood out by displaying the highest specific activity towards 4-HB: UGT75B1 (At1g05560), which glucosylates the carboxyl group to form the glucose ester of 4-HB, and UGT89B1 (At1g73880) and UGT71B1 (At3g21750), which glucosylate at the *para* position to give the 4-*O*-glucoside conjugate (Lim et al. 2002). Since glycosylation is the major metabolic fate of 4-HB in Arabidopsis tissues, we investigated the contribution of each of these three UGTs in vivo. To do that, T-DNA lines corresponding to insertions in exonic regions of UGT75B1, UGT89B1, and UGT71B1 were isolated, confirmed (Fig. S2), and levels of glycosylated, free, and cell wall-bound 4-HB were determined in the corresponding mutants (Fig. 4). Since in all plant species tested so far, including within the Brassicaceae family, glycosylated 4-HB has been found to occur mainly as monoglycosyl conjugates (Cooper-Driver et al. 1972), we posited that loss of function of a major UGT would result in an increase in the ratio of free 4-HB to glycosylated 4-HB. In rosette leaves and flowers, none of the T-DNA lines displayed any statistically significant differences in the proportions of 4-HB as compared to the wild-type controls (Fig. 4a, b). The flowers of the *ugt71b1* mutant contained about twice as much free 4-HB than their wild-type counterparts, but

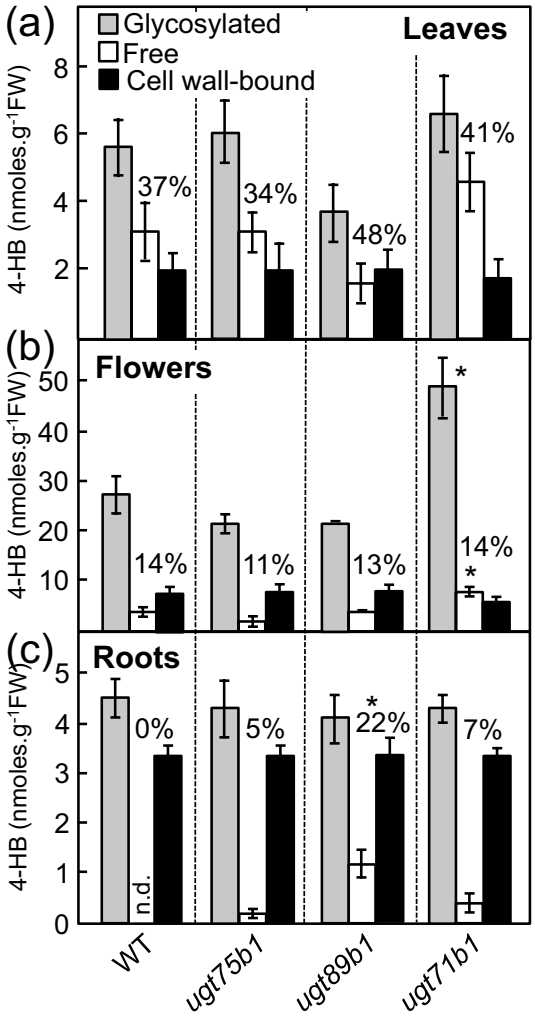

Fig. 4 Content in glycosylated, free, and cell wall-bound 4-HB in wild-type and UGT mutant *ugt75b1*, *ugt89b1*, and *ugt71b1* Arabidopsis plants. **a** Leaves; **b** flowers; **c** roots. Percentages indicate the percent of free 4-HB out of soluble 4-HB. Data represent the means of 4 biological replicates ± SE. Asterisks indicate significant differences from the wild-type control as determined by Fisher's test ($p < 0.1$) from an analysis of variance

such an increase was paralleled by a similar increase in glycosyl conjugates. In roots, traces of free 4-HB were detected in the *ugt75b1* and *ugt71b1* T-DNA lines, while it was not detected in the wild-type control (Fig. 4c). The proportion of free 4-HB in the roots of the *ugt89b1* T-DNA line, however, was significantly higher than that of the other mutants, representing approximately a quarter of the total pool of soluble 4-HB (Fig. 4c). These results suggest that UGT75B1, UGT89B1, and UGT71B1 play only a marginal role in the glycosylation of 4-HB in vivo. Functional redundancies within the UGT family could explain such a result. Along this line, five additional Arabidopsis UGTs are known to moonlight on 4-HB in vitro; two of these (UGT84A1 and UGT75B2) are capable of forming 4-HB glucose ester, and the other three (UGT78D2, UGT73B3, UGT73B4) the 4-HB-*O*-glucoside (Lim et al. 2002).

Conclusions

Keeping in mind that At4g19010, 4-CL8, and F3H are connected via a common pool of *p*-coumarate (Fig. 1), and therefore, that the metabolic impact of knocking-out one or two of the cognate genes can be mitigated via an increase in biosynthetic flux through the remaining functional enzyme(s), the following conclusions can be drawn. i) The pool sizes of glycosylated and free 4-HB can vary vastly between organs. In contrast, the proportion of cell wall-bound 4-HB is relatively constant. ii) The respective contributions of the β-oxidation of *p*-coumarate and of kaempferol cleavage to the different pools of 4-HB depend on the organs, and so does the contribution of the two 4-coumaroyl-CoA ligases within the β-oxidative branch. For instance, 4-CL8 bears a preponderant role in the production of soluble and cell wall-bound 4-HB in leaves, while At4g19010 appears to be the controlling ligase for the biosynthesis of soluble 4-HB in flowers. Similarly, the proportion of kaempferol-derived 4-HB is higher in roots than in leaves and flowers. iii) The *at4g19010*×*f3h* double knockout consistently displays the most severe decrease in total 4-HB content as compared to the other mutants, indicating that the β-oxidation of *p*-coumarate and the peroxidative catabolism of kaempferol both contribute to the supply of 4-HB in leaves, flowers, and roots. It is important to note, however, given the myriad of phenylpropanoid-derived compounds occurring throughout plant taxa and the large variations in the sizes of the associated metabolic pools and fluxes (Weng and Chapple 2010; Tohge et al. 2013), that some of the features of 4-HB metabolism reported here for Arabidopsis could be vastly different in other species. This is particularly so for woody taxa, in which the pool size of lignin-bound 4-HB in mature xylem can be at least 4 orders of magnitude larger (Mottiar et al. 2023) than that we measured in Arabidopsis tissues. Last, our findings suggest that the major UGTs that are involved in the glycosylation of 4-HB in Arabidopsis tissues, both for the formation of the corresponding glucose ester and 4-*O*-glucoside conjugates, remain to be identified.

Supplementary Information The online version contains supplementary material available at https://doi.org/10.1007/s00425-024-04572-2.

Acknowledgements This work was made possible in part by National Science Foundation Grant MCB-2216747 (to G.J.B.) and by USDA-Agricultural Research Service project 6036-11210-001-000D (to AKB).

Author contributions Z.B. designed and performed the experiments, analyzed the data and wrote the manuscript. G.J.B. designed

the experiments, analyzed the data and wrote the manuscript. A.B. designed and performed the experiments, and analyzed the data.

Data availability The experimental data that support the findings of this study are available upon request.

Declarations

Conflict of interest The authors declare no conflict of interest.

References

Alonso JM, Stepanova AN, Leisse TJ, Kim CJ, Chen H, Shinn P, Stevenson DK, Zimmerman J, Barajas P, Cheuk R, Gadrinab C, Heller C, Jeske A, Koesema E, Meyers CC, Parker H, Prednis L, Ansari Y, Choy N, Deen H, Geralt M, Hazari N, Hom E, Karnes M, Mulholland C, Ndubaku R, Schmidt I, Guzman P, Aguilar-Henonin L, Schmid M, Weigel D, Carter DE, Marchand T, Risseeuw E, Brogden D, Zeko A, Crosby WL, Berry CCE, Ecker JR (2003) Genome-Wide insertional mutagenesis of *Arabidopsis thaliana*. Science 301:653–657. https://doi.org/10.1126/science.1086391

Berger A, Latimer S, Stutts LR, Soubeyrand E, Block AK, Basset GJ (2022) Kaempferol as a precursor for ubiquinone (coenzyme Q) biosynthesis: an atypical node between specialized metabolism and primary metabolism. Curr Opin Plant Biol 66:102165. https://doi.org/10.1016/j.pbi.2021.102165

Block A, Widhalm JR, Fatihi A, Cahoon RE, Wamboldt Y, Elowsky C, Mackenzie SA, Cahoon EB, Chapple C, Dudareva N, Basset GJ (2014) The origin and biosynthesis of the benzenoid moiety of ubiquinone (Coenzyme Q) in Arabidopsis. Plant Cell 26:1938–1948. https://doi.org/10.1105/tpc.114.125807

Cooper-Driver G, Corner-Zamodits JJ, Swain T (1972) The metabolic fate of hydroxybenzoic acids in plants. Z Naturforsch 27 b:943–946. https://doi.org/10.1515/znb-1972-0817

Dawson RMC, Elliot DC, Elliot WH, Jones KM (1986) Data for biochemical research. Oxford University Press, New York

Goacher RE, Mottiar Y, Mansfield SD (2021) ToF-SIMS imaging reveals that p-hydroxybenzoate groups specifically decorate the lignin of fibres in the xylem of poplar and willow. Holzforschung 75:452–462. https://doi.org/10.1515/hf-2020-0130

Lim EK, Doucet CJ, Li Y, Elias L, Worrall D, Spencer SP, Ross J, Bowles DJ (2002) The activity of Arabidopsis glycosyltransferases toward salicylic acid, 4-hydroxybenzoic acid, and other benzoates. J Biol Chem 277:586–692. https://doi.org/10.1074/jbc.M109287200

Lu F, Karlen SD, Regner M, Kim H, Ralph SA, Sun R-C, Kuroda K-I, Augustin MA, Mawson R, Sabarez H, Singh T, Jimenez-Monteon G, Zakaria S, Hill S, Harris PJ, Boerjan W, Wilkerson CG, Mansfield SD, Ralph J (2015) Naturally p-Hydroxybenzoylated Lignins in Palms. Bioenerg Res 8:934–952. https://doi.org/10.1007/s12155-015-9583-4

Masini L (2014) Investigation of the molecular basis of PAMP-induced resistance. Dissertation, University of East Anglia, The Sainsbury Laboratory, Norwich, United-Kingdom

Mottiar Y, Karlen SD, Goacher RE, Ralph J, Mansfield SD (2023) Metabolic engineering of p-hydroxybenzoate in poplar lignin. Plant Biotechnol J 21:176–188. https://doi.org/10.1111/pbi.13935

Nakanishi K, Li H, Ichino T, Tatsumi K, Osakabe K, Watanabe B, Shimomura K, Yazaki K (2024) Peroxisomal 4-coumaroyl-CoA ligases participate in shikonin production in *Lithospermum erythrorhizon*. Plant Physiol Kiae. https://doi.org/10.1093/plphys/kiae157

Pierrel F (2017) Impact of chemical analogs of 4-hydroxybenzoic acid on coenzyme Q biosynthesis: from inhibition to bypass of coenzyme Q deficiency. Front Physiol 8:436. https://doi.org/10.3389/fphys.2017.00436

Rencoret J, Marques G, Serrano O, Kaal J, Martínez AT, del Río JC, Gutiérrez A (2020) Deciphering the Unique Structure and Acylation Pattern of *Posidonia oceanica* Lignin. ACS Sustain Chem Eng 8:12521–12533. https://doi.org/10.1021/acssuschemeng.0c03502

Siebert M, Sommer S, Li SM, Wang ZX, Severin K, Heide L (1996) Genetic engineering of plant secondary metabolism. Accumulation of 4-hydroxybenzoate glucosides as a result of the expression of the bacterial *ubi*C gene in tobacco. Plant Physiol 112:811–819. https://doi.org/10.1104/pp.112.2.811

Soubeyrand E, Johnson TS, Latimer S, Block A, Kim J, Colquhoun TA, Butelli E, Martin C, Wilson MA, Basset GJ (2018) The peroxidative cleavage of kaempferol contributes to the biosynthesis of the benzenoid moiety of ubiquinone in plants. Plant Cell 30:2910–2921. https://doi.org/10.1105/tpc.18.00688

Soubeyrand E, Kelly M, Keene SA, Bernert AC, Latimer S, Johnson TS, Elowsky C, Colquhoun TA, Block AK, Basset GJ (2019) Arabidopsis 4-COUMAROYL-COA LIGASE 8 contributes to the biosynthesis of the benzenoid ring of coenzyme Q in peroxisomes. Biochem J 476:3521–3532. https://doi.org/10.1042/BCJ20190688

Soubeyrand E, Latimer S, Bernert AC, Keene SA, Johnson TS, Shin D, Block AK, Colquhoun TA, Schäffner AR, Kim J, Basset GJ (2021) 3-*O*-glycosylation of kaempferol restricts the supply of the benzenoid precursor of ubiquinone (Coenzyme Q) in *Arabidopsis thaliana*. Phytochemistry 186:112738. https://doi.org/10.1016/j.phytochem.2021.112738

Suttiyut T, Benzinger SW, McCoy RM, Widhalm JR (2023) Strategies to study the metabolic origins of specialized plant metabolites: the specialized 1,4-naphthoquinones. Methods Enzymol 680:217–246. https://doi.org/10.1016/bs.mie.2022.08.020

Tohge T, Watanabe M, Hoefgen R, Fernie AR (2013) The evolution of phenylpropanoid metabolism in the green lineage. Crit Rev Biochem Mol Biol 48:123–152. https://doi.org/10.3109/10409238.2012.758083

Viitanen PV, Devine AL, Khan MS, Deuel DL, Van Dyk DE, Daniell H (2004) Metabolic engineering of the chloroplast genome using the *Escherichia coli ubi*C gene reveals that chorismate is a readily abundant plant precursor for p-hydroxybenzoic acid biosynthesis. Plant Physiol 136:4048–4060. https://doi.org/10.1104/pp.104.050054

Weng JK, Chapple C (2010) The origin and evolution of lignin biosynthesis. New Phytol 187:273–285. https://doi.org/10.1111/j.1469-8137.2010.03327.x

Xue JS, Zhang B, Zhan H, Lv YL, Jia XL, Wang T, Yang NY, Lou YX, Zhang ZB, Hu WJ, Gui J, Cao J, Xu P, Zhou Y, Hu JF, Li L, Yang ZN (2020) Phenylpropanoid derivatives are essential components of sporopollenin in vascular plants. Mol Plant 13:1644–1653. https://doi.org/10.1016/j.molp.2020.08.005

Yazaki K (2017) *Lithospermum erythrorhizon* cell cultures: Present and future aspects. Plant Biotechnol (Tokyo) 34:131–142. https://doi.org/10.5511/plantbiotechnology.17.0823a

Yazaki K, Inushima K, Kataoka M, Tabata M (1995) Intracellular localization of UDPG: p -Hydroxybenzoate glucosyltransferase and its reaction product in *Lithospermum* cell cultures. Phytochemistry 38:1127–1130. https://doi.org/10.1016/0031-9422(94)00821-A